VOL. 15, NO. 16, AUGUST 2020 ISSN 1819-6608
ARPN Journal of Engineering and Applied Sciences

www.arpnjournals.com

UNDERSTANDING OF CORROSION IN GAS PIPELINES OF API 5L X65 THROUGH CHARACTERIZING SLUDGE FORMED

A. R. S. Nurhidayat, A. Suprihanto and A. P. Bayuseno
Department of Mechanical Engineering, Faculty of Engineering, Diponegoro University, Campus Tembalang, Semarang, Indonesia
E-Mail: Akhlisrahman22@gmail.com

ABSTRACT

Natural gas with acid gases (H_2S, CO_2, and organic acids) transported in the pipeline leads to a corrosion process and produces sludge accumulated in the pipe. This study was devoted to understanding the corrosion of API 5L X65 pipelines by examining the resulting sludge. The collected sludge was then treated and dried to become powder. Subsequently, the powder was subjected to XRF, XRD and SEM-EDX analysis for experimental material characterization. The obtained sludge contains major elements of Fe, Ca, Mn, and S according to the XRF analysis, while the resulting particle shape was in the form of rounded, irregular aggregates with a size of 8.427 µm and 6.775 µm while EDX results show the most chemical composition of specimens corresponding to elements of Fe, C, and O. The XRD Rietveld method confirmed that magnetite (Fe_3O_4) is the main crystalline mineral found in the corrosion product, while some minor products (e.g.$CaCO_3$, $FeCO_3$, and FeS) could be not detected under detecting limit of x-ray diffraction study. Evidently, the pipelines of API 5L X65 had been subjected to mainly CO_2 corrosion, but a further assessment of this mechanism is still needed for a failure prediction and corrosion protection program of pipelines.

Keywords: pipelines of API 5L X65; sludge; SEM; XRF; XRD Rietveld method.

INTRODUCTION

Oil and gas are transported on pipelines always accompanying some water, carbon dioxide, hydrogen sulfide, and organic acids, which can vary in amounts. Moreover, the presence of these chemical compounds may dissolve in water and react electrochemically to the iron of steel, which leads to internal corrosion. In the petroleum and gas industries, the corrosion of a mild steel pipe can lead to serious problems that need a prediction, inhibition and inspection/monitoring management system. Even many steel alloys having good corrosion resistance can be used, economics is the main consideration of mild steel selection for pipelines, which has become so far the most economical material. Additionally, the corrosion mechanism may lead the failure material, hence eventually contributing to the higher direct and higher indirect costs, relating to the production costs of oil and gases.

Basically, corrosion of the mild metal occurs when exposed to aqueous environments containing aggressive substances (e.g. water and gas). Specifically, water chemistry in crude oil wells and in natural gas wells contains salt contributing corrosion. Moreover, gases CO_2 and H_2S available in natural gas have good solubility in the pure water leading to becoming acidic and corrosive. Because of its solubility in water and brine, the sweet corrosion can be developed in the carbon steel, while the presence of H_2S leads to sour corrosion. Also, O_2 could be a corrosive gas to steel. Here corrosion rate and its intensity on carbon steel are influenced by the character and concentration of aggressive ingredients, pressure, temperature, flow regime, and velocity.

Pressure, temperature, and pH influencing on the internal corrosion of pipe have been well documented [1]–[6]. The gases of H_2S, CO_2, and H_2O is dissolved in water depending on pressure and temperature and control the corrosion rate [7]–[9]. In particular, the corrosion product in the presence of CO_2 dissolved in water may form $FeCO_3$ scale [10–12]. Moreover, the corrosion products that can be formed in $CO_2/H_2S/H_2O/Fe_2O_3$ systems include iron carbonate (FeCO3) and iron sulfides (FexSy). When oxygen is not present in the fluids, iron oxides maybe not formed. Here the iron carbonate can be formed according to:

$$Fe^{2+}_{(aq)} + CO^{2-}_{3(aq)} \Leftrightarrow FeCO_{3(s)} \quad (1)$$

Under thermodynamic condition, scaling of mild steel occurs in the supersaturated solution (>1) as follows:

$$S_{FeCO_3} = \frac{[Fe^{2+}][CO_3^{2-}]}{K_{spFeCO3}} \quad (2)$$

In spite of the degree of super-saturation, the scaling rate of the steel depends on temperature. The process of deposition on the surface of the material influences the presence of a scaling mechanism and allows it to form a protective layer. Here to understand the exact mechanisms of internal corrosion needs to check different factors influencing the CO_2 corrosion rate through the characterization experiments on the sludge produced.

This present paper provided experimental results of the sludge characteristic of natural gas flowing in pipes. The experimental characterization included the chemical composition of pipes, phase and morphology analysis utilizing XRF, XRD and SEM-EDX method respectively. The study can be used to complement the integrity management of the pipeline for sustainable production.

MATERIALS AND METHODS

Materials of Sludge Examined in the Study

The pipe material of API 5L X65 employed in the plant has compositions (wt.%) of 0.11% C, 0.48% Si,

1.58% Mn, 0.06% Cr, 0.18% Mo, 0.01% Cu, 0.061%, Fe balance, while the composition of the gases transporting in the pipeline is presented in Table-1. The pressure of the gas flowing at 2.97 MPa and a temperature of 45 ^{O}C is commonly operated. Obviously methane is the main gas containing natural gas observed in the study.

Further sludge investigated was collected from the pigging process during the maintenance time monthly in Central Java, Indonesia (Figure-1). In this way, the sludge still mixed with condensate was then be left in the bottle open and allowed to dry under the sunlight. Here the condensate has acidity at pH 5. Eventually, the dried Sludge was manually sieved using mesh 8 and subsequently subjected to XRF investigation (Figure-1 b).

Table-1. Natural gas composition.

Gas Composition	Mole percent (%)
Methane	93.5099
Nitrogen	0.4889
Carbon Dioxide	0.0009
Ethane	3.4775
Propane	1.2270
H_2O	0.0009
H_2S	0.0066
i-butane	0.2693
n-butane	0.3550
i-pentane	0.1312
n-pentane	0.1197
n-hexane	0.4584

Table-2. Composition of XRF test sludge.

Element	*Sludge Powder* (wt.%)
Al	0.0876
Si	0.837
P	0.0326
S	1.28
Cl	0.0422
K	0.0972
Ca	1.31
Mn	1.27
Fe	94.3
Nb	0.026
Mo	0.096
Hg	0.615

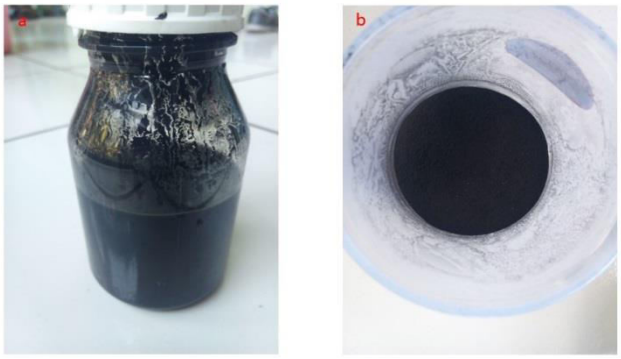

Figure-1. (a) Sludge mixing with condensate (b) Powder of the dried sludge.

Materials Characterization

Chemical elements of the dried sludge was determined by Energy Dispersive X-ray Fluorescence (EDXRF). Particle chemistry and morphology of the treated sludge was also examined by SEM-EDX (JEOL JSM-6510LA). SEM images were collected by a Mega view III digital camera (EMSIS GmbH). Prior to SEM/EDX examinations, specimens were glued together with sticky tape on a circular Al-sample holder and finally sputtered with carbon.

X-ray diffraction (XRD) data were collected for mineral identification using Cu-K (monochromated radiation (Bragg-Brentano geometry, SHIMADZU X-Ray Diffractometer). The recorded data were used for a PC-based search match program to indicate the crystalline phases against the data of the International Centre for Diffraction Data-Powder Diffraction File (ICDD-PDF). The suggested phases were then verified by the Rietveld method (FullProf-2k software version 3.30). For the Rietveld refinement, the crystal structure model was taken from the literature of the American mineralogist crystal structure database (AMCSD).

RESULTS AND DISCUSSIONS

Bulk-Chemistry of the Dried Sludge

Chemical compositions of the dried sludge were examined for major and trace elements (Table-2). These bulk chemical compositions of the sludge powders were determined by XRF method. The constituents are provided in terms of elements (wt. %), unrelated to the real chemical compounds in the dried sludge. Here chemical elements of oxygen and carbon are not shown. But, the ions with a positive charge (cations) could be joined to form with oxides, silicates, and sulfates. Chemical elements (>1 wt. %) in the specimens collected from the sludge are Fe2+, Ca2+, Sn+, and Mn+, while minor concentrations of Si-, Cl+, and Al3+. Furthermore, the major chemical element of the sludge with large Fe-metal scraps removed is considered to be similar to rust, which would be verified by the XRD method.

Particle Chemistry and Morphology

The electrochemical process has strong effects on corrosion mechanisms resulting in particle chemistry, and morphology of the sludge. In this regard, particle morphology and size are important aspects that control the corrosion behavior of the sludge. Varying morphological shapes and chemical elements of the sludge was investigated by SEM equipped with EDX (Figures 2 and 3). The majority of the sludge particles were angular-shaped, porous aggregates (in the range of 8.427 µm and 6.775 µm) µm in diameter, with a flaky morphology. Spherical particles were not observed in the sludge. The angular and/or porous aggregates in the sludge containing inorganic constituents that were bound and the porosity was developed because of the O_2 and CO_2 losses. The most common elements identified by EDX in the particles are Fe, Ca, S, and Si, similar findings with the bulk compositions determined by XRF. Kα-the peak of oxygen and Kα-peaks of carbon were found in the EDX spectra of particles. These constituents were occasionally found with Fe-rich oxide particles. Moreover, the large particle aggregates may also contain two or more phases (i.e. glass and crystalline phase). The rusts may be also produced by H_2S and CO_2 which is affected by pressure and temperature has an irregular shape particle [16].

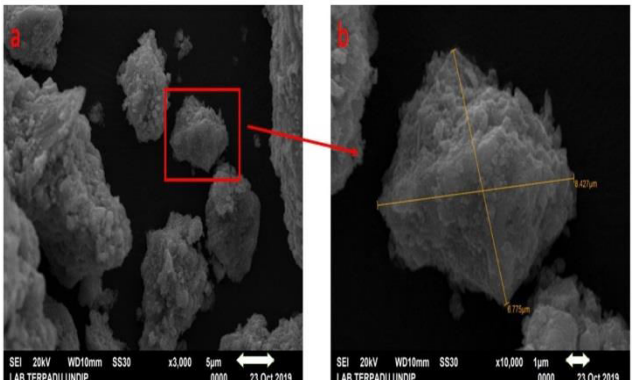

Figure-2. (a) Angular shape and (b) Particle size of the powder sludge.

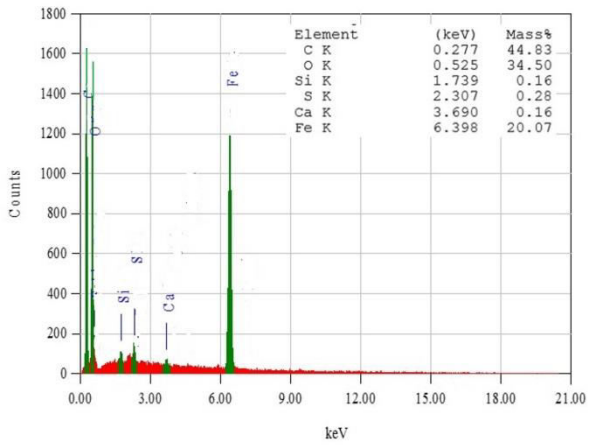

Figure-3. Semi-quantitative analysis of sludge powder.

The semi-quantitative analysis of EDX was performed on the corrosion product of the sample shown in Figure-3. The elements consisting of 20.7 % Fe mass, 44.83% mass C, and 34.5% mass may provide one of the corrosion products forming FeO, Fe_2O_3, or $FeCO_3$ [17].

Mineralogical Phase Analysis of the Sludge

The mineralogical characteristics of the dried sludge were examined to identify the major phases controlling the O_2 and CO_2 corrosion. The XRD Rietveld method confirmed that the specimen contains mainly magnetite (Fe_3O_4) as a result of CO_2 corrosion (Figure-4), while the iron carbonate ($FeCO_{3)}$ may be present in a minor concentration in addition to some impurity minerals (e.g. $CaCO_3$ and $FeCO_3$), which can be inferred from SEM-EDX analysis (Figure-3).

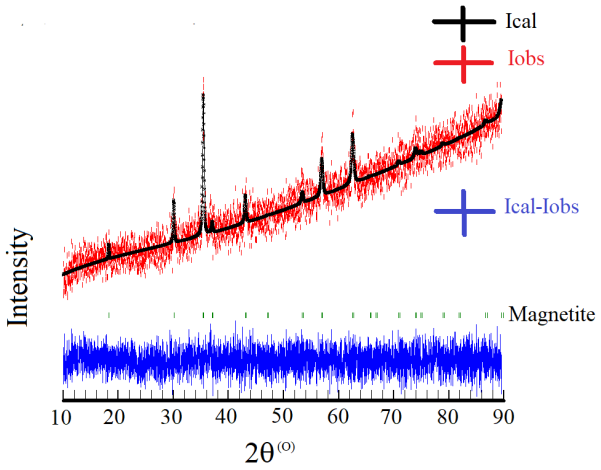

Figure-4. The plot of the XRD Rietveld pattern-fitting results for the specimens, confirming magnetite present. The observed profile intensities (Iobs) and the calculated profile intensities (Ical) were fitted very well showing in the bottom curve.

Apparently, the CO_2 corrosion as a result of the heterogeneous electrochemical reactions had occurred inside pipelines [13, 14]. Here iron oxide (magnetite) was probably formed at higher temperatures (T > 100 OC) in CO2 aqueous solutions and cooled to room temperature. This formation of magnetite might be also supported by the pH solution, while the corrosion rate occurred rapidly resulting in thin (<1 µm) and inert deposits, which would stick tightly to the steel surface. Moreover, the formation of magnetite deposits was accompanied by one order of magnitude or more for the reduced corrosion rates. However, some magnetite could be formed even at lower temperatures (<100 OC). This magnetite might be not detected since its product layer is found in cavities and pores with small amounts, which also contribute to the overall protectiveness [15, 16].

Further, more complex surface deposits might be formed on pipes which can be results of other salts precipitating and controlling the corrosion rate. The possible minerals may include iron sulfides and iron carbonates forming in H_2S and CO_2 dissolved solutions.

Other possibilities of scales (calcium carbonate) are formed in the sludge observed during the study. These scales formed in the sludge may also control the corrosion protection of metal surfaces.

Importantly, the CO_2 corrosion observed in the study occurred possibly via two main mechanisms, the homogeneous (in the solution near the metal surface) and heterogeneous chemical reactions (mass transfer from the bulk solution). Here temperature, and pH control CO_2 corrosion corresponding to the CO_2 content. However further work including failure prediction and the extension of design and implementation for the appropriate mitigation program of corrosion should be performed [17].

CONCLUSIONS

This study analyses the effect of corrosion on the sludge which was influenced by temperature and pressure on natural gas transportation. It can be concluded that;

a) H_2S, CO_2, and H_2O were carried by natural gas along pipeline caused corrosion which forms a sludge with a dominant element in the form of Fe.
b) The morphology of the sludge was identified as an irregular shape with a length of 8.427 µm and a width of 6.775 µm. In a semi-quantitative analysis, there is a dominant element besides Fe, in the form of elements C and O.
c) Major mineral of magnetite (Fe_3O_4) was found as a corrosion product confirmed by XRD Rietveld method, in addition to minor minerals such as calcite ($CaCO_3$) and $FeCO_3$, which could be predicted by SEM-EDX analysis.

ACKNOWLEDGMENT

The authors would like to the Indonesian Natural Gas Industry for providing the sludge specimens and Diponegoro University for performing the XRD, XRF and SEM-EDX experiments.

REFERENCE

[1] H. Zhang, Y. L. Zhao and Z. D. Jiang. 2005. Effects of temperature on the corrosion behavior of 13Cr martensitic stainless steel during exposure to CO 2 and Cl - environment. Mater. Lett. 59(27): 3370-3374.

[2] W. Sun, S. Nešić and R. C. Woollam. 2009. The effect of temperature and ionic strength on iron carbonate (FeCO3) solubility limit. Corros. Sci. 51(6): 1273-1276.

[3] P. Sui *et al.* 2018. Effect of temperature and pressure on corrosion behavior of X65 carbon steel in water-saturated CO2 transport environments mixed with H2S. Int. J. Greenh. Gas Control. 73(November 2017): 60-69.

[4] G. A. Zhang and Y. F. Cheng. 2011. Localized corrosion of carbon steel in a CO2-saturated oilfield formation water. Electrochim. Acta. 56(3): 1676-1685.

[5] Y. Zhang, X. Pang, S. Qu, X. Li, and K. Gao. 2012. Discussion of the CO 2 corrosion mechanism between low partial pressure and supercritical condition. Corros. Sci. 59: 186-197.

[6] S. Nešić. 2007. Key issues related to modelling of internal corrosion of oil and gas pipelines - A review. Corrosion Science. 49(12): 4308-4338.

[7] R. Barker, D. Burkle, T. Charpentier, H. Thompson and A. Neville. 2018. A review of iron carbonate (FeCO3) formation in the oil and gas industry. Corros. Sci. 142(July): 312-341.

[8] Y. Hua, R. Barker and A. Neville. 2015. Comparison of corrosion behaviour for X-65 carbon steel in supercritical CO2-saturated water and water-saturated/unsaturated supercritical CO2. J. Supercrit. Fluids. 97: 224-237.

[9] R. A. De Motte, R. Barker, D. Burkle, S. M. Vargas and A. Neville. 2018. The early stages of FeCO3 scale formation kinetics in CO2 corrosion. Mater. Chem. Phys. 216: 102-111.

[10] S. Guo, L. Xu, L. Zhang, W. Chang and M. Lu. 2016. Characterization of corrosion scale formed on 3Cr steel in CO2-saturated formation water. Corros. Sci. 110: 123-133.

[11] Z. Jia, X. Li, C. Du, Z. Liu and J. Gao. 2012. Effect of the carbon dioxide pressure on the electrochemical behavior of 3Cr low alloyed steel at high temperature. Mater. Chem. Phys. 136(2-3): 973-979.

[12] C. Bian, Z. M. Wang, X. Han, C. Chen and J. Zhang. 2015. Electrochemical response of mild steel in ferrous ion enriched and CO2 saturated solutions. Corros. Sci. 96: 42-51.

[13] Y. Hua, A. Shamsa, R. Barker and A. Neville. 2018. Protectiveness, morphology and composition of corrosion products formed on carbon steel in the presence of Cl -, Ca 2+ and Mg 2+ in high pressure CO 2 environments. Appl. Surf. Sci. 455(May): 667-682.

[14] D. Burkle *et al*. 2017. In situ SR-XRD study of FeCO 3 precipitation kinetics onto carbon steel in CO 2 -

containing environments: The influence of brine pH. Electrochim. Acta. 255: 127-144.

[15] L. Wei, X. Pang, C. Liu and K. Gao. 2015. Formation mechanism and protective property of corrosion product scale on X70 steel under supercritical CO 2 environment. Corros. Sci. 100: 404-420.

[16] C. Sun, J. Sun, Y. Wang, X. Lin, X. Li and X. Cheng. 2016. Synergistic effect of O2, H2S and SO2 impurities on the corrosion behavior of X65 steel in water-saturated supercritical CO 2 system. Eval. Program Plann. 107: 193-203.

[17] E. Latosov, B. Maaten, A. Siirde and A. Konist. 2018. The influence of O2 and CO2 on the possible corrosion on steel transmission lines of natural gas. Energy Procedia. 147: 63-70.